DNA methylomes derived from alveolar macrophages display distinct patterns in latent tuberculosis - implication for interferon gamma release assay status determination

Isabelle Pehrson[1ð], Jyotirmoy Das[1ð], Nina Idh[1], Lovisa Karlsson[1], Helena Rylander[1], Hilma Hård af Segerstad[1], Elsa Reuterswärd[1], Emma Marttala[1], Jakob Paues[1,2], Melissa Méndez-Aranda[3], César Ugarte-Gil[4•], and Maria Lerm[1•*]

[1]Division of Inflammation and Infection, [2]Division of Infectious Diseases, Department of Biomedical and Clinical Sciences, Faculty of Medicine and Health Sciences, Linköping University, SE-58185, Linköping, Sweden, [3]Facultad de Ciencias y Filosofía, Laboratorio de Investigación en Enfermedades Infecciosas, [4]Facultad de Medicina; Instituto de Medicina Tropical Alexander von Humboldt, Universidad Peruana Cayetano Heredia, Peru

ð*) Shared first authorship*

•*) Shared last authorship*

***) Corresponding author:**

Maria Lerm, Div. of Inflammation and Infection, Lab 1, floor 12

Dept. of Biomedical and Clinical Sciences, Faculty of Medicine and Health Sciences

Linköping University, SE-58185 Linköping, Sweden

Phone: +46-732707786, E-mail: maria.lerm@liu.se

Keywords: DNA methylation, tuberculosis, LTBI, IGRA, sputum induction, epigenetics

Abstract

Host innate immune cells, including alveolar macrophages, have been identified as key players in the early eradication of *Mycobacterium tuberculosis* and in the maintenance of an anti-mycobacterial immune memory, which is believed to be induced through epigenetic changes. The aim of the study was to elucidate whether exposure to *M. tuberculosis* induced a different DNA methylation pattern of alveolar macrophages and pulmonary T lymphocytes.

Alveolar macrophages and T lymphocytes were isolated from induced sputum obtained from individuals living in Lima, which is an area high endemic for tuberculosis. To determine the latent tuberculosis infection status of the subjects, an interferon-γ release assay was performed. We evaluated the DNA methylomes of the alveolar macrophages and T lymphocytes using the Illumina Infinium Human Methylation 450K Bead Chip array, revealing a distinct DNA methylation pattern in alveolar macrophages allowing the discrimination of asymptomatic individuals with latent tuberculosis infection from non-infected individuals. Pathway analysis revealed that cell signalling of inflammation and chemokines in alveolar macrophages play a role in latent tuberculosis infection. In conclusion, we demonstrated that DNA methylation in alveolar macrophages can be used to determine the tuberculosis infection status of individuals in a high endemic setting.

Introduction

Infection with *Mycobacterium tuberculosis*, the causative agent of tuberculosis (TB), can result in active disease or latent infection. Globally, two billion individuals are currently estimated to have a latent TB infection (LTBI), and 5-15% of those will develop active TB during their lifetime [1-4]. In the rest of TB-exposed individuals, the innate immune system will eliminate the bacteria before the onset of an adaptive immune response, with no detectable evidence of a persistent immune response, referred to as early clearance [5,6].

M. tuberculosis is primarily transmitted via airborne droplets and inhaled into the airways where it establishes an infection that could develop into pulmonary TB [1]. When *M. tuberculosis* reaches the alveoli within the lungs, the pathogen is phagocytosed by alveolar macrophages, a subgroup of lung tissue-resident macrophages, which form part of the innate immune system and are among the first host cells that the bacteria encounter [7,8]. Subsequently, lung T lymphocytes are recruited and begin to engage in immune responses against the pathogen [8,9].

The only TB-vaccine available today is the *M. bovis* Bacillus Calmette-Guèrin (BCG). The vaccine is effective in protecting infants and small children against miliary TB and meningitis but is unsuccessful in protecting adults against pulmonary TB [10,11]. In addition to its protective effect against TB in children, the vaccine also protects them against unrelated pathogens and even reduce general mortality in children, which could be explained by epigenetic reprogramming of innate immune cells, referred to as trained immunity [12-16]. The trained innate immune system is in part regulated by DNA methylation, an epigenetic modifier which regulates various processes within the cell, including anti-inflammatory responses [17,18].

For the diagnosis of LTBI, the best options today are the tuberculin skin test (TST) and interferon-γ (IFN-γ) release assay (IGRA) [1,19]. The IGRAs detect IFN-γ secondary to T lymphocyte activation and secretion as a response to exposure to *M. tuberculosis*-specific proteins. The IGRA T-SPOT.*TB* has shown a high reproducibility in serial testing and to have higher sensitivity than other available tests [20,21].

LTBI is a dynamic state that can progress to active tuberculosis under immunesenescence or immunosuppression, since it reflects a balance between host immune responses and the bacilli. Thus, LTBI can be viewed as a spectrum, with variable levels of bacterial control and risk of progression to active TB infection [22-24]. Even though attempts have been made to identify biomarkers of LTBI and LTBI progression, including DNA methylation events in peripheral immune cells of active and latent TB patients [25,26], no study to our knowledge has investigated DNA methylation in cells of the lung compartment of IGRA-positive latently infected individuals.

Biosignatures of TB have been proposed to lay ground for next generation of diagnostics for TB [27,28] and accumulating literature have been published studying possible TB biosignatures, based on e.g., global methylation analysis, transcriptional profiling and RNA sequencing enrichment [29-32]. However, no biomarker or signature of active or latent TB has been successful when generalized or applied in larger sample sizes and biosignature based diagnostics tools are still unavailable in the clinic.

In this study, we isolated alveolar macrophages from individuals residing in a Lima, Peru which has a high prevalence of tuberculosis. We performed DNA methylation analyses to identify changes in the methylome and detected 265 significant differently methylated CpG sites (DMCs) when comparing individuals with LTBI with IGRA-negative non-TB (NTB)

85 individuals. Further analysis of the DMCs revealed their importance in several pathways of
86 the innate immune system.

Methods

Ethical approval

Ethical approval was obtained from the Institutional Committee on Research Ethics "Comité Institucional de Ética en Investigación" (CIEI) of the Cayetano Heredia National Hospital, Nº 082-018 for the inclusion of patients and Universidad Peruana Cayetano Heredia Institutional Review Board Nº 101773 for the inclusion of healthy subjects.

Subjects

Peru has a high prevalence of TB and a heavy burden of multidrug-resistant (MDR) and extensively drug-resistant (XDR) TB [33,34]. With reference to the increased risk of Peruvian health care workers and medical students to acquire a TB infection [35-38], subjects were recruited from the from the Universidad Peruana Cayetano Heredia (UPCH) and the Hospital Nacional Cayetano Heredia in Lima, Peru during April, October and November 2018. 26 individuals aged 18-40 years were included in the study following oral and written consent. Based on the IGRA results, the subjects were divided into IGRA-positives (LTBI group) and IGRA-negatives (here defined as NTB group). DNA from alveolar macrophages and T lymphocytes, obtained via sputum induction, were isolated from both groups and the number of differentially methylated CpG-sites (DMCs) assessed. For the alveolar macrophages, pathway analysis and cluster analysis were performed. An auxiliary heatmap analysis was performed with the addition of two drug resistant tuberculosis (DRTB) patients, included in June 2019. Following cell isolation and DNA extraction, one HLA-DR and one CD3 sample from two different subjects (both NTB) had to be excluded due to insufficient DNA amount.

IFN-γ release assay

The latent TB infection status of all subjects except for the active TB patients was evaluated with an IGRA. The TB infection status of the active TB patients was based on current

111 medical records. Following venepuncture, the IGRA (T-SPOT.*TB*, Oxford Immunotec) was
112 performed, measuring the IFN-γ release of the peripheral immune cells, per the
113 manufacturer's protocol. The T-SPOT.*TB* result is based on the number of spot-forming cells
114 (memory T cells producing IFN-γ, sensitized in response to the mycobacterial antigens
115 ESAT-6 and CFP-10).

116 ***Sputum induction and processing***

117 Sputum specimen were collected and processed as previously described [39], with some
118 modifications. The lung immune cells were obtained from each subject (here, salbutamol was
119 avoided) after the nebulization of a hypertonic saline solution (4%) three times, provoking a
120 profound cough via osmosis, producing pulmonal secretions. The coughing was preceded by
121 an oral cleaning procedure. After the collection of the expectorate via sputum induction, the
122 cell-rich samples were transferred to various cell-culture dishes and accumulations of mucus
123 of immune cells, referred to as "plugs", were transferred to tubes using forceps. Following
124 the plug collection, the volume of the sample was estimated and a solution containing
125 phosphate buffer solution (PBS) and 0.1% dithiothreitol (DTT) was added to the sample
126 equal to four times the volume of the sample, to provide a reducing agent to decrease sample
127 viscosity. Following this, the sample was diluted with PBS, and rocked for 5 minutes before
128 filtrated through a 50 µm cell strainer into a new tube to remove contaminating squamous
129 cells and centrifuged for 5 minutes.

130 ***DNA extraction of isolated alveolar macrophages and T lymphocytes***

131 Sikkeland *et al.* have previously described the method for the isolation of HLA-DR positive
132 alveolar macrophages [39,40]. The alveolar macrophages and T lymphocytes (CD3 positive
133 cells) were isolated according to our protocol [39] using superparamagnetic beads coupled with
134 anti-human CD3 and Pan Mouse IgG antibodies and HLA-DR/human MHC class II

antibodies (Invitrogen Dynabeads). An initial positive selection was done with CD3 beads followed by a positive HLA-DR selection. Bead coating and cell isolation was performed according to manufacturer's protocol. The DNA and RNA were extracted from the lung immune cells using the AllPrep DNA/RNA Mini Kit (Qiagen), per the manufacturer's instructions, and quantified using the spectrophotometer NanoDrop 2000/2000c (Thermo Scientific).

DNA methylation data analysis

Genome-wide DNA methylation analysis of the DNA from the two cell types (HLA-DR and CD3 positive cells) was performed using the Infinium Human Methylation 450K Bead Chip array (Illumina) as per the manufacturer's instructions. The technique is based on quantitative genotyping of C/T polymorphism which is generated by DNA bisulfite conversion and allows for the assessment of over 450 000 methylation sites within the whole genome. DNA was converted and amplified and subsequently fragmented and hybridized to the Infinium HumanMethylation450 Bead Chip. The procedure was conducted at the Karolinska Institute, Sweden.

Computational analysis

The IDAT files (RAW files that contain green and red signals from methylated and unmethylated CpG sites) were analyzed using the R programming language (v3.6.3) (R Foundation for Statistical Computing: Vienna, Austria) and Chip Analysis Methylation Pipeline (*ChAMP*) analysis package [41]. The following filters were applied: i) detection of *p*-value (<0.01), ii) remove non-CpG probes, iii) SNP removal, iv) remove multi-hit probes, v) remove all probes in X and Y chromosomes [41]. After filtering, quality control was performed, and normalization of the data was made using the BMIQ method. The β-values and M-values of the samples were calculated against each probe per sample. Differential methylation

159 analysis of CpG sites (DMCs) between the sample groups was then performed using
160 Bonferroni-Hochberg (BH)-corrected *p*-value ($p\text{-value}_{BH}$) < 0.05. The DMCs were annotated
161 with the Illumina manifest file using GRCh37/hg19 database.

162 The statistically significant ($p\text{-value}_{BH}$ < 0.05) was used to create the static volcano plot with
163 the |log2FC| ≥0.3 using the *EnhancedVolcano plot* package package [42] in R. The hierarchical
164 cluster analyses were performed from the β-values of the significant DMCs from each
165 participant using the *hclust* function of the *ade4/ape* package [43] in R. The R packages
166 *ComplexHeatmap* [44] was used to create the heatmap from individual β-values of DMCs (*p*-
167 value_{BH} < 0.05 and $\log_2$ fold change ≥ |0.4|). For the CD3 positive cells we found 0 DMCs (*p*-
168 value_{BH} < 0.05) (not shown) and thus no other analyses were performed on the CD3 positive
169 cells. The design matrix of the DNA methylation analysis was "LTBI - NTB" meaning that a
170 positive $\log_2$ fold change value equals hypermethylated DMC in the LTBI group. Negative
171 $\log_2$ fold change value means NTB DMCs are hypermethylated. Pathway enrichment analysis
172 was performed using Signaling Pathway Impact Analysis (SPIA) [45] enrichment analysis and
173 *pathfindR* [46], based on information from the Kyoto Encyklopedia of Genes and Genomes
174 (KEGG) [47]. Via the SPIA enrichment analysis, based on pathway information from KEGG,
175 we used the expression rates of the LTBI vs NTB DMGs to calculate signaling pathway
176 topology. The R package *pathfindR* is a tool for pathway enrichment analyses that uses active
177 subnetwork to calculate the pathway enrichment. Using the enriched DMGs separating the
178 LTBI from NTB, we identified active subnetworks and performed pathway enrichment
179 analyses on the identified subnetworks. Via a scoring function, the overall activity of each
180 pathway in each sample was estimated.

Results

Subject characteristics

In order to identify possible DMCs to reflect TB-exposure, we included healthy subjects with presumable high and low exposure to TB residing in a high endemic area in Lima, Peru and subsequently divided into two groups based on their IGRA result (Fig. 1). Among the healthy subjects that were included, six we identified as IGRA-positive (LTBI) and 19 as IGRA-negative individuals (NTB). Demographics, body metrics, Bacillus Calmette-Guèrin (BCG)- and smoking status are summarized in Table 1. The patients (DRTB) were hospitalized and were suffering from MDR-TB and XDR-TB, respectively (Table 2). One patient was smear microscopy positive and suffered from cough, dyspnea, and night sweats while the other was asymptomatic and smear microscopy negative at the time. One patient had received the MDR-antibiotic regimen since 2016. The other patient had a TB disease history of over 10 years, with susceptible TB since 2008 and a later progression to MDR-TB (2016) and XDR-TB (2019). Both patients were treated with multiple antibiotics at the time of inclusion.

Differential DNA methylation analysis identified DMCs to distinguish LTBI from NTB in alveolar macrophages

To determine whether LTBI and NTB can be distinguished based on the methylation pattern, we compared the alveolar macrophage and T lymphocyte DNA methylome data obtained from LTBI and NTB subjects. The analysis revealed 265 DMCs with a $p\text{-value}_{BH} < 0.05$ and $\log_2$ fold change value $\geq|0.3|$ for alveolar macrophages (not shown). The DMCs differentiating LTBI from NTB are presented as DMCs with their equivalent DMGs in a volcano plot (Fig. 2).

In total, 36 055 DMCs was found to distinguish LTBI from NTB without any $\log_2$ fold change value cut-off (not shown). The same DNA methylation analysis performed with the

lung T lymphocytes resulted in 0 DMCs (p-value$_{BH}$ < 0.05) (not shown). Thus, no further analysis was performed on the T lymphocytes. No DMCs were found between the subjects included as TB-exposed and non-exposed (not shown).

A heatmap analysis revealed a distinct DNA methylation pattern of LTBI and drug resistant TB in alveolar macrophages

After demonstrating that the LTBI and NTB groups had distinct DNA methylation traits, knowing that heterogenicity of the epigenome of LTBI subjects has previously been demonstrated [48] and that LTBI can be viewed as a spectrum [22], we performed a heatmap analysis based on the top DMCs of the DNA methylation analysis (265 DMCs, p-value$_{BH}$ <0.05, $\log_2$ fold change ≥|0.3|) that showed that the LTBI group, with the exception of one participant, clustered into one group (Fig. 3a). In order to investigate whether we could identify any TB-like subjects within the diverse LTBI group, as previously demonstrated by Estévez *et al.* [48], we recruited two individuals with TB and with ongoing treatment to the study (Table 2). The cluster analysis revealed that the DRTB group clustered with the 5 LTBI subjects (Fig. 3a). A subsequent principal component analysis (PCA, Fig. 3b) revealed that the DRTB, despite the similarities with the LTBI group in the cluster analysis, formed a separate population, demonstrating that the three conditions are clearly separated by the identified DNA methylation signature.

Biological processes involved in latent tuberculosis infection

Next, we investigated the biological processes involved in LTBI, based on the genes found in the differential DNA methylation analysis. We performed pathway enrichment analyses of the alveolar macrophages to identify the common pathways that distinguished the LTBI samples from the NTB and found pathways involved in the spliceosome, Wnt signaling, mTOR signaling, regulation of actin cytoskeleton, ribosome, extracellular matrix

229 organization, MAPK signaling, cellular senescence, TGF-β signaling and the
230 phosphatidylinositol signaling system (Fig. 4).

231 In addition, SPIA pathway enrichment analysis was performed, corroborating the enrichment
232 of innate immune-related pathways, including chemokine signaling pathway, antigen
233 processing and presentation, *Staphylococcus aureus* infection, the NOD-like receptor
234 signaling pathway and intestinal immune network for IgA production (Table S1).

235 ***Counter DNA methylation status of genes persistently hypomethylated in BCG responders***

236 In our previous study, PBMCs obtained from BCG-vaccinated individuals, whose
237 macrophages displayed an enhanced anti-mycobacterial response, displayed persistent
238 hypomethylation in six genes, among them the gene encoding IFN-γ [49]. In order to estimate
239 whether these genes' DNA methylation status of the BCG study was coherent with the LTBI
240 data in the present study, we compared the β values of these genes in the different studies.
241 Contrary to the observations in the BCG vaccinees, the six genes were found to be
242 hypermethylated in LTBI (Table S2).

Discussion

In this study, we found that five out of six individuals diagnosed with LTBI based on a positive IGRA displayed a distinct DNA methylation pattern of alveolar macrophages. The reason why one of the LTBI individual's signature aligned with the NTB group remains obscure, but it is tempting to speculate that this individual had cleared a previous latent TB infection, allowing the LTBI-specific DNA methylome signature to fade while the adaptive immune memory against TB antigens endured. However, further studies are needed to provide evidence for such a relationship. A limitation with the present study is that no information on previous IGRA test results was available, and future studies will dissect the relationship between the timing of IGRA conversion and the intensity of the DNA methylome signature.

In our previous study on DNA methylation alterations in response to the BCG vaccine, we identified CpG sites in six gene promoters, one of which belonging to the *IFNG* gene (encoding IFN-γ), as being persistently more accessible for transcription (hypomethylated) in BCG responders. In contrast, the present study showed that the very same six CpG sites were hypermethylated in the LTBI group [49]. We hypothesize that the transcription accessibility of these six genes has importance for the clearance of *M. tuberculosis*, reflective of a beneficial BCG response [49]. LTBI is a manifestation of lost mycobacterial control by innate mechanisms and possibly a consequence of hypermethylation of for example IFN-γ, which has a non-disputable importance for the control of TB [50].

While being a risk factor for developing active TB, LTBI has been shown to convey protection against *M. tuberculosis* reinfection, partly explained by heterologous immunity and the concomitant activation of the innate immune system [51,52]. The protective mechanisms of LTBI were associated with activation of alveolar macrophages and accelerated recruitment

of *M. tuberculosis*-specific T cells to the lung and enhanced cytokines production [52], compatible with our results where we showed an overrepresentation of pathways involved in TGF-β, NOD-like receptor (NLR) and chemokine signaling. The activation of the NLRP3 inflammasome, activated via *NLRP3* promotor demethylation, has previously been identified as an important regulatory function in TB [53]. Interestingly, *NLRP3* was differentially methylated between the LTBI and NTB at 3 CpG sites in our data and we identified NLR signaling as an activated pathway in LTBI. Increased NLPR3 inflammasome activation enhances the anti-mycobacterial capacity of macrophages [54] and prevents development of active pulmonary TB [55].

Methylation of the *VDR* promoter (regulating Vitamin D receptor expression) has previously been demonstrated to be of importance in TB [56-58], especially for disease progression and risk. Vitamin D enhances macrophage capacity to control intracellular *M. tuberculosis* [59,60]. In our data, we found three differentially methylated *VDR* CpG sites, all hypermethylated in the LTBI group, pointing towards downregulation of VDR responsiveness in alveolar macrophages from subjects with LTBI, which may impair their ability to kill intracellular mycobacteria [61].

Early clearance is observed in about 25% of individuals who are living with considerable exposure to TB [62-64], and epigenetic mechanisms related to trained immunity could contribute to the elimination of the infection without any need to trigger an adaptive immune response [65]. We propose that the LTBI group has been unsuccessful in clearing the bacteria and that the epigenetic differences we identify between the LTBI and NTB group.

The heatmap analysis revealed that the DNA methylation pattern of alveolar macrophages of DRTB patients, who were on MDR treatment at the timepoint of inclusion, displayed similar pattern with the LTBI individuals, however they formed a distinct cluster the PCA analysis.

Since the DRTB patients had been on TB treatment for an extended period of time, our study does not reveal the DNA methylome signature of active pulmonary TB, but suggests that DNA methylome analysis is a promising approach to study the spectrum of TB. Therefore, longitudinal studies are needed that cover DNA methylation changes of alveolar macrophages before the time point of IGRA conversion over the development of active TB and the TB treatment until cure. The results will allow dissection of the unique DNA methylation signatures for each state of TB and could be further developed as tools for clinical TB diagnosis, decision-making in LTBI infected subjects and TB treatment monitoring.

Data and materials availability

Sequencing datasets will be made publicly available upon acceptance and prior to final publication.

Acknowledgements

We owe our thanks to the Bioinformatics and Expression Analysis core facility (BEA), which is supported by the board of research at the Karolinska Institute and the research committee at the Karolinska hospital. The study was funded through a grant from the Swedish Research Council N^{o} 2018-04246 and the Consejo Nacional de Ciencia, Tecnología e Innovación Tecnológica CONCYTEC and Cienciactiva (N^{o} 106-2018-FONDECYT). The computations and data handling were enabled by resources provided by the Swedish National Infrastructure for Computing (SNIC) at National Supercomputing Centre (NSC), Linköping University partially funded by the Swedish Research Council through grant agreement N^{o} 2018-05973. We also owe thanks to the support by grants from the World Infection Fund. J.D is a postdoctoral fellow supported through the Medical Infection and Inflammation Center (MIIC) at Linköping University. We direct our gratitude to all the subjects for donating samples. We are also grateful for the help of Ronald Cadillo Hernandez and Rodrigo Cachay Figueroa.

Authors Contribution

M.L, N.I, J.P, C.U-G and M.M-A wrote the ethical application and conceived the study. I.P, E.M, H.R, E.R and H.H performed all sample collections. J.D and L.K preformed the bioinformatic analyses. I.P, M.L, J.D and L.K wrote the manuscript. M.M-A and C.U-G supervised the project in Peru.

Conflicting interest

All authors declare no conflict of interest.

Consent for publication

All authors have approved to the final version of the manuscript.

References

1. WHO | Global tuberculosis report 2020. WHO. Geneva, Switzerland. 2020

2. Vynnycky E, Fine PE. The natural history of tuberculosis: the implications of age-dependent risks of disease and the role of reinfection. Epidemiol Infect. 1997 Oct;119(2):183-201. doi: 10.1017/s0950268897007917.

3. Comstock GW, Livesay VT, Woolpert SF. The prognosis of a positive tuberculin reaction in childhood and adolescence. Am J Epidemiol. 1974 Feb;99(2):131-8. doi: 10.1093/oxfordjournals.aje.a121593.

4. Sester M, van Leth F, Bruchfeld J, Bumbacea D, Cirillo DM, Dilektasli AG, Domínguez J, Duarte R, Ernst M, Eyuboglu FO, Gerogianni I, Girardi E, Goletti D, Janssens JP, Julander I, Lange B, Latorre I, Losi M, Markova R, Matteelli A, Milburn H, Ravn P, Scholman T, Soccal PM, Straub M, Wagner D, Wolf T, Yalcin A, Lange C; TBNET. Risk assessment of tuberculosis in immunocompromised patients. A TBNET study. Am J Respir Crit Care Med. 2014 Nov 15;190(10):1168-76. doi: 10.1164/rccm.201405-0967OC.

5. Meermeier EW, Lewinsohn DM. Early clearance versus control: what is the meaning of a negative tuberculin skin test or interferon-gamma release assay following exposure to Mycobacterium tuberculosis? F1000Res. 2018 May 25;7:F1000 Faculty Rev-664. doi: 10.12688/f1000research.13224.1.

6. Koeken VACM, Verrall AJ, Netea MG, Hill PC, van Crevel R. Trained innate immunity and resistance to Mycobacterium tuberculosis infection. Clin Microbiol Infect. 2019 Dec;25(12):1468-1472. doi: 10.1016/j.cmi.2019.02.015. Epub 2019 Feb 23.

7. Cohen SB, Gern BH, Delahaye JL, Adams KN, Plumlee CR, Winkler JK, Sherman DR, Gerner MY, Urdahl KB. Alveolar Macrophages Provide an Early Mycobacterium tuberculosis Niche and Initiate Dissemination. Cell Host Microbe. 2018 Sep 12;24(3):439-446.e4. doi: 10.1016/j.chom.2018.08.001. Epub 2018 Aug 23.

8. Mayer-Barber KD, Barber DL. Innate and Adaptive Cellular Immune Responses to Mycobacterium tuberculosis Infection. Cold Spring Harb Perspect Med. 2015 Jul 17;5(12):a018424. doi: 10.1101/cshperspect.a018424.

9. Eghtesad M, Jackson HE, Cunningham AC. Primary human alveolar epithelial cells can elicit the transendothelial migration of CD14+ monocytes and CD3+ lymphocytes. Immunology. 2001 Feb;102(2):157-64. doi: 10.1046/j.1365-2567.2001.01172.x.

10. Roy A, Eisenhut M, Harris RJ, Rodrigues LC, Sridhar S, Habermann S, Snell L, Mangtani P, Adetifa I, Lalvani A, Abubakar I. Effect of BCG vaccination against Mycobacterium tuberculosis infection in children: systematic review and meta-analysis. BMJ. 2014 Aug 5;349:g4643. doi: 10.1136/bmj.g4643.

11. Mangtani P, Abubakar I, Ariti C, Beynon R, Pimpin L, Fine PE, Rodrigues LC, Smith PG, Lipman M, Whiting PF, Sterne JA. Protection by BCG vaccine against tuberculosis: a systematic review of randomized controlled trials. Clin Infect Dis. 2014 Feb;58(4):470-80. doi: 10.1093/cid/cit790. Epub 2013 Dec 13.

12. Butkeviciute E, Jones CE, Smith SG. Heterologous effects of infant BCG vaccination: potential mechanisms of immunity. Future Microbiol. 2018 Aug;13(10):1193-1208. doi: 10.2217/fmb-2018-0026. Epub 2018 Aug 17.

13. Ferluga J, Yasmin H, Al-Ahdal MN, Bhakta S, Kishore U. Natural and trained innate immunity against Mycobacterium tuberculosis. Immunobiology. 2020 May;225(3):151951. doi: 10.1016/j.imbio.2020.151951. Epub 2020 Apr 27.

14. Netea MG, Joosten LA, Latz E, Mills KH, Natoli G, Stunnenberg HG, O'Neill LA, Xavier RJ. Trained immunity: A program of innate immune memory in health and disease. Science. 2016 Apr 22;352(6284):aaf1098. doi: 10.1126/science.aaf1098. Epub 2016 Apr 21.

15. Arts RJW, Moorlag SJCFM, Novakovic B, Li Y, Wang SY, Oosting M, Kumar V, Xavier RJ, Wijmenga C, Joosten LAB, Reusken CBEM, Benn CS, Aaby P, Koopmans MP, Stunnenberg HG, van Crevel R, Netea MG. BCG Vaccination Protects against Experimental Viral Infection in Humans through the Induction of Cytokines Associated with Trained Immunity. Cell Host Microbe. 2018 Jan 10;23(1):89-100.e5. doi: 10.1016/j.chom.2017.12.010.

16. Covián C, Fernández-Fierro A, Retamal-Díaz A, Díaz FE, Vasquez AE, Lay MK, Riedel CA, González PA, Bueno SM, Kalergis AM. BCG-Induced Cross-Protection and Development of Trained Immunity: Implication for Vaccine Design. Front Immunol. 2019 Nov 29;10:2806. doi: 10.3389/fimmu.2019.02806.

17. Maruthai K, Kalaiarasan E, Joseph NM, Parija SC, Mahadevan S. Assessment of global DNA methylation in children with tuberculosis disease. Int J Mycobacteriol. 2018 Oct-Dec;7(4):338-342. doi: 10.4103/ijmy.ijmy_107_18.

18. Morales-Nebreda L, McLafferty FS, Singer BD. DNA methylation as a transcriptional regulator of the immune system. Transl Res. 2019 Feb;204:1-18. doi: 10.1016/j.trsl.2018.08.001. Epub 2018 Aug 9.

19. Furin J, Cox H, Pai M. Tuberculosis. Lancet. 2019 Apr 20;393(10181):1642-1656. doi: 10.1016/S0140-6736(19)30308-3. Epub 2019 Mar 20.

20. Meier T, Enders M. High reproducibility of the interferon-gamma release assay T-SPOT.TB in serial testing. Eur J Clin Microbiol Infect Dis. 2021 Jan;40(1):85-93. doi: 10.1007/s10096-020-03997-3. Epub 2020 Aug 8.

21. Pai M, Zwerling A, Menzies D. Systematic review: T-cell-based assays for the diagnosis of latent tuberculosis infection: an update. Ann Intern Med. 2008 Aug 5;149(3):177-84. doi: 10.7326/0003-4819-149-3-200808050-00241. Epub 2008 Jun 30.

22. Barry CE 3rd, Boshoff HI, Dartois V, Dick T, Ehrt S, Flynn J, Schnappinger D, Wilkinson RJ, Young D. The spectrum of latent tuberculosis: rethinking the biology and intervention strategies. Nat Rev Microbiol. 2009 Dec;7(12):845-55. doi: 10.1038/nrmicro2236. Epub 2009 Oct 26.

23. Chee CBE, Reves R, Zhang Y, Belknap R. Latent tuberculosis infection: Opportunities and challenges. Respirology. 2018 Oct;23(10):893-900. doi: 10.1111/resp.13346. Epub 2018 Jun 14.

24. Drain PK, Bajema KL, Dowdy D, Dheda K, Naidoo K, Schumacher SG, Ma S, Meermeier E, Lewinsohn DM, Sherman DR. Incipient and Subclinical Tuberculosis: a Clinical Review of Early Stages and Progression of Infection. Clin Microbiol Rev. 2018 Jul 18;31(4):e00021-18. doi: 10.1128/CMR.00021-18.

25. Esterhuyse MM, Weiner J 3rd, Caron E, Loxton AG, Iannaccone M, Wagman C, Saikali P, Stanley K, Wolski WE, Mollenkopf HJ, Schick M, Aebersold R, Linhart H, Walzl G, Kaufmann SH. Epigenetics and Proteomics Join Transcriptomics in the

Quest for Tuberculosis Biomarkers. mBio. 2015 Sep 15;6(5):e01187-15. doi: 10.1128/mBio.01187-15.

26. Sharma G, Sowpati DT, Singh P, Khan MZ, Ganji R, Upadhyay S, Banerjee S, Nandicoori VK, Khosla S. Genome-wide non-CpG methylation of the host genome during M. tuberculosis infection. Sci Rep. 2016 Apr 26;6:25006. doi: 10.1038/srep25006.

27. Haas CT, Roe JK, Pollara G, Mehta M, Noursadeghi M. Diagnostic 'omics' for active tuberculosis. BMC Med. 2016 Mar 23;14:37. doi: 10.1186/s12916-016-0583-9.

28. Lerm M, Dockrell HM. Addressing diversity in tuberculosis using multidimensional approaches. J Intern Med. 2018 May 27. doi: 10.1111/joim.12776. Epub ahead of print.

29. Maertzdorf J, Kaufmann SH, Weiner J 3rd. Toward a unified biosignature for tuberculosis. Cold Spring Harb Perspect Med. 2014 Oct 23;5(1):a018531. doi: 10.1101/cshperspect.a018531.

30. Petrilli JD, Araújo LE, da Silva LS, Laus AC, Müller I, Reis RM, Netto EM, Riley LW, Arruda S, Queiroz A. Whole blood mRNA expression-based targets to discriminate active tuberculosis from latent infection and other pulmonary diseases. Sci Rep. 2020 Dec 16;10(1):22072. doi: 10.1038/s41598-020-78793-2.

31. Pan L, Wei N, Jia H, Gao M, Chen X, Wei R, Sun Q, Gu S, Du B, Xing A, Zhang Z. Genome-wide transcriptional profiling identifies potential signatures in discriminating active tuberculosis from latent infection. Oncotarget. 2017 Dec 4;8(68):112907-112916. doi: 10.18632/oncotarget.22889.

32. Zheng L, Leung ET, Wong HK, Lui G, Lee N, To KF, Choy KW, Chan RC, Ip M. Unraveling methylation changes of host macrophages in Mycobacterium tuberculosis infection. Tuberculosis (Edinb). 2016 May;98:139-48. doi: 10.1016/j.tube.2016.03.003. Epub 2016 Mar 21.

33. Alarcón V, Alarcón E, Figueroa C, Mendoza-Ticona A. Tubersulosis en el Perú: situación epidemiológica, avances y desafíos para su control [Tuberculosis in Peru: epidemiological situation, progress and challenges for its control]. Rev Peru Med Exp Salud Publica. 2017 Apr-Jun;34(2):299-310. Spanish. doi: 10.17843/rpmesp.2017.342.2384.

34. Woodman M, Haeusler IL, Grandjean L. Tuberculosis Genetic Epidemiology: A Latin American Perspective. Genes (Basel). 2019 Jan 16;10(1):53. doi: 10.3390/genes10010053.

35. Pérez-Lu JE, Cárcamo CP, García PJ, Bussalleu A, Bernabé-Ortiz A. Tuberculin skin test conversion among health sciences students: a retrospective cohort study. Tuberculosis (Edinb). 2013 Mar;93(2):257-62. doi: 10.1016/j.tube.2012.10.001. Epub 2012 Oct 30.

36. Baussano I, Nunn P, Williams B, Pivetta E, Bugiani M, Scano F. Tuberculosis among health care workers. Emerg Infect Dis. 2011 Mar;17(3):488-94. doi: 10.3201/eid1703.100947.

37. Soto-Cabezas MG, Chávez-Pachas AM, Arrasco-Alegre JC, Yagui-Moscoso MJ. Tuberculosis en trabajadores de salud en el Perú, 2013-2015 [Tuberculosis in health workers in Peru, 2013-2015]. Rev Peru Med Exp Salud Publica. 2016 Oct-Dec;33(4):607-615. Spanish. doi: 10.17843/rpmesp.2016.334.2542.

38. Soto Cabezas MG, Munayco Escate CV, Chávez Herrera J, López Romero SL, Moore D. Prevalencia de infección tuberculosa latente en trabajadores de salud de establecimientos del primer nivel de atención. Lima, Perú [Prevalence of latent tuberculosis infection in health workers from primary health care centers in Lima, Peru]. Rev Peru Med Exp Salud Publica. 2017 Oct-Dec;34(4):649-654. Spanish. doi: 10.17843/rpmesp.2017.344.3035.

39. Das J, Idh N, Sikkeland L. I. B, Paues J, Lerm M. DNA methylome-based validation of induced sputum as an effective protocol to study lung immunity: construction of a classifier of pulmonary cell types. bioRxiv (2021) doi:10.1101/2021.03.12.435086

40. Sikkeland LI, Kongerud J, Stangeland AM, Haug T, Alexis NE. Macrophage enrichment from induced sputum. Thorax. 2007 Jun;62(6):558-9. doi: 10.1136/thx.2006.073544.

41. Morris TJ, Butcher LM, Feber A, Teschendorff AE, Chakravarthy AR, Wojdacz TK, Beck S. ChAMP: 450k Chip Analysis Methylation Pipeline. Bioinformatics. 2014 Feb 1;30(3):428-30. doi: 10.1093/bioinformatics/btt684. Epub 2013 Dec 12.

42. Blighe K, Rana S, Lewis M (2020). EnhancedVolcano: Publication-ready volcano plots with enhanced colouring and labeling. R package version 1.8.0, https://github.com/kevinblighe/EnhancedVolcano.

43. Paradis E, Schliep K (2019). “ape 5.0: an environment for modern phylogenetics and evolutionary analyses in R.” Bioinformatics, 35, 526-528.

44. Gu Z, Eils R, Schlesner M (2016). “Complex heatmaps reveal patterns and correlations in multidimensional genomic data.” Bioinformatics.

45. Tarca AL, Kathri P, Draghici S (2020). SPIA: Signaling Pathway Impact Analysis (SPIA) using combined evidence of pathway over-representation and unusual signaling perturbations. R package version 2.42.0, http://bioinformatics.oxfordjournals.org/cgi/reprint/btn577v1.

46. Ulgen E, Ozisik O, Sezerman OU. pathfindR: An R Package for Comprehensive Identification of Enriched Pathways in Omics Data Through Active Subnetworks. Front Genet. 2019 Sep 25;10:858. doi: 10.3389/fgene.2019.00858.

47. KEGG as a reference resource for gene and protein annotation Nucleic Acids Research, Volume 44, Issue D1, 4 January 2016, Pages D457–D462, https://doi.org/10.1093/nar/gkv1070

48. Estévez O, Anibarro L, Garet E, Pallares Á, Barcia L, Calviño L, Maueia C, Mussá T, Fdez-Riverola F, Glez-Peña D, Reboiro-Jato M, López-Fernández H, Fonseca NA, Reljic R, González-Fernández Á. An RNA-seq Based Machine Learning Approach Identifies Latent Tuberculosis Patients With an Active Tuberculosis Profile. Front Immunol. 2020 Jul 14;11:1470. doi: 10.3389/fimmu.2020.01470.

49. Verma D, Parasa VR, Raffetseder J, Martis M, Mehta RB, Netea M, Lerm M. Anti-mycobacterial activity correlates with altered DNA methylation pattern in immune cells from BCG-vaccinated subjects. Sci Rep. 2017 Sep 26;7(1):12305. doi: 10.1038/s41598-017-12110-2.

50. Moreira-Teixeira L, Mayer-Barber K, Sher A, O'Garra A. Type I interferons in tuberculosis: Foe and occasionally friend. J Exp Med. 2018 May 7;215(5):1273-1285. doi: 10.1084/jem.20180325. Epub 2018 Apr 17.

51. Andrews JR, Noubary F, Walensky RP, Cerda R, Losina E, Horsburgh CR. Risk of progression to active tuberculosis following reinfection with Mycobacterium

tuberculosis. Clin Infect Dis. 2012 Mar;54(6):784-91. doi: 10.1093/cid/cir951. Epub 2012 Jan 19.

52. Nemeth J, Olson GS, Rothchild AC, Jahn AN, Mai D, Duffy FJ, Delahaye JL, Srivatsan S, Plumlee CR, Urdahl KB, Gold ES, Aderem A, Diercks AH. Contained Mycobacterium tuberculosis infection induces concomitant and heterologous protection. PLoS Pathog. 2020 Jul 16;16(7):e1008655. doi: 10.1371/journal.ppat.1008655.

53. Wei M, Wang L, Wu T, Xi J, Han Y, Yang X, Zhang D, Fang Q, Tang B. NLRP3 Activation Was Regulated by DNA Methylation Modification during Mycobacterium tuberculosis Infection. Biomed Res Int. 2016;2016:4323281. doi: 10.1155/2016/4323281. Epub 2016 Jun 6.

54. Eklund D, Welin A, Andersson H, Verma D, Söderkvist P, Stendahl O, Särndahl E, Lerm M. Human gene variants linked to enhanced NLRP3 activity limit intramacrophage growth of Mycobacterium tuberculosis. J Infect Dis. 2014 Mar 1;209(5):749-53. doi: 10.1093/infdis/jit572. Epub 2013 Oct 24.

55. Souza de Lima D, Ogusku MM, Sadahiro A, Pontillo A. Inflammasome genetics contributes to the development and control of active pulmonary tuberculosis. Infect Genet Evol. 2016 Jul;41:240-244. doi: 10.1016/j.meegid.2016.04.015. Epub 2016 Apr 19.

56. Andraos C, Koorsen G, Knight JC, Bornman L. Vitamin D receptor gene methylation is associated with ethnicity, tuberculosis, and TaqI polymorphism. Hum Immunol. 2011 Mar;72(3):262-8. doi: 10.1016/j.humimm.2010.12.010. Epub 2010 Dec 16.

533 57. Jiang C, Zhu J, Liu Y, Luan X, Jiang Y, Jiang G, Fan J. The methylation state of
534 VDR gene in pulmonary tuberculosis patients. J Thorac Dis. 2017 Nov;9(11):4353-
535 4357. doi: 10.21037/jtd.2017.09.107.

536 58. Wang M, Kong W, He B, Li Z, Song H, Shi P, Wang J. Vitamin D and the
537 promoter methylation of its metabolic pathway genes in association with the risk
538 and prognosis of tuberculosis. Clin Epigenetics. 2018 Sep 12;10(1):118. doi:
539 10.1186/s13148-018-0552-6.

540 59. Chen L, Eapen MS, Zosky GR. Vitamin D both facilitates and attenuates the
541 cellular response to lipopolysaccharide. Sci Rep. 2017 Mar 27;7:45172. doi:
542 10.1038/srep45172.

543 60. Eklund D, Persson HL, Larsson M, Welin A, Idh J, Paues J, Fransson SG, Stendahl
544 O, Schön T, Lerm M. Vitamin D enhances IL-1β secretion and restricts growth of
545 Mycobacterium tuberculosis in macrophages from TB patients. Int J
546 Mycobacteriol. 2013 Mar;2(1):18-25. doi: 10.1016/j.ijmyco.2012.11.001. Epub
547 2012 Dec 20.

548 61. Liu PT, Stenger S, Li H, Wenzel L, Tan BH, Krutzik SR, Ochoa MT, Schauber J,
549 Wu K, Meinken C, Kamen DL, Wagner M, Bals R, Steinmeyer A, Zügel U, Gallo
550 RL, Eisenberg D, Hewison M, Hollis BW, Adams JS, Bloom BR, Modlin RL. Toll-
551 like receptor triggering of a vitamin D-mediated human antimicrobial response.
552 Science. 2006 Mar 24;311(5768):1770-3. doi: 10.1126/science.1123933. Epub
553 2006 Feb 23.

554 62. Hill PC, Brookes RH, Fox A, Jackson-Sillah D, Jeffries DJ, Lugos MD, Donkor
555 SA, Adetifa IM, de Jong BC, Aiken AM, Adegbola RA, McAdam KP.

Longitudinal assessment of an ELISPOT test for Mycobacterium tuberculosis infection. PLoS Med. 2007 Jun;4(6):e192. doi: 10.1371/journal.pmed.0040192.

63. Stein CM, Zalwango S, Malone LL, Thiel B, Mupere E, Nsereko M, Okware B, Kisingo H, Lancioni CL, Bark CM, Whalen CC, Joloba ML, Boom WH, Mayanja-Kizza H. Resistance and Susceptibility to Mycobacterium tuberculosis Infection and Disease in Tuberculosis Households in Kampala, Uganda. Am J Epidemiol. 2018 Jul 1;187(7):1477-1489. doi: 10.1093/aje/kwx380.

64. Verrall AJ, Alisjahbana B, Apriani L, Novianty N, Nurani AC, van Laarhoven A, Ussher JE, Indrati A, Ruslami R, Netea MG, Sharples K, van Crevel R, Hill PC. Early Clearance of Mycobacterium tuberculosis: The INFECT Case Contact Cohort Study in Indonesia. J Infect Dis. 2020 Mar 28;221(8):1351-1360. doi: 10.1093/infdis/jiz168.

65. Verrall AJ, Schneider M, Alisjahbana B, Apriani L, van Laarhoven A, Koeken VACM, van Dorp S, Diadani E, Utama F, Hannaway RF, Indrati A, Netea MG, Sharples K, Hill PC, Ussher JE, van Crevel R. Early Clearance of Mycobacterium tuberculosis Is Associated With Increased Innate Immune Responses. J Infect Dis. 2020 Mar 28;221(8):1342-1350. doi: 10.1093/infdis/jiz147.

573 **Figure legends**

574 **Figure 1.** A flow chart of the study design. TB = tuberculosis. IGRA = interferon-γ release
575 assay. LTBI = latent tuberculosis infection. NTB = non-tuberculosis. DRTB = drug resistant
576 tuberculosis. DMCs = differentially methylated CpG-sites.

577 **Figure 2**. Volcano plot of the differentially methylated CpG-sited (DMCs) separating the
578 latent tuberculosis infection (LTBI) from the non-tuberculosis (NTB) group. The plot is
579 showing the distribution of the DMCs fold changes in LTBI relative to NBT in alveolar
580 macrophages. Each dot represents one CpG site (p-value$_{BH} < 0.05$). x-scale = $\log_2$FC, y-scale
581 = $-\log_{10}$ p adjusted; blue CpGs = hypomethylated; red CpGs = hypermethylated; black CpGs
582 = significant but $|\log_2 FC|<0.3$ horizontal black line in parallel to x-axis = p-value$_{BH} < 0.05$,
583 and vertical green lines parallel to y-axis = $|\log_2 FC| \geq 0.3$.

584 **Figure 3a.** Heatmap of the LTBI, NTB and DRTB groups. The heatmap is plotted from
585 the β-values of the top 265 CpGs ($\log_2$ fold change $\geq|0.3|$, p-value$_{BH} < 0.05$) differentiating
586 the LTBI and NTB groups. The drug-resistant TB patients (DR-TB) are added to the
587 analysis. The color scale represent the β-value (from 0 (blue) to 1 (red)) of each CpG site.
588 Orange: LTBI = latent tuberculosis infection, green: NTB = non-tuberculosis, red: DRTB =
589 drug-resistant tuberculosis as shown in the bar plot of the heatmap. Cluster dendrogram is
590 calculated using the Euclidean distance method.

591 **Figure 3b.** Principal components analysis (PCA) of the LTBI, NTB and DRTB group. The
592 PCA plot is generated from the β-values of the top 265 CpGs ($\log_2$ fold change $\geq|0.3|$, p-
593 value$_{BH} < 0.05$) differentiating the LTBI and NTB groups, with the addition of the β-
594 values of the DRTB patients of those DMCs.

595 **Figure 4.** Top 10 clusters of the enriched pathways from pathfindR based on the
596 differentially methylated genes (DMGs) differentiating LTBI from NTB. The dot plot is

597 demonstrating the most relevant pathways for the alveolar macrophages when comparing the
598 LTBI with the NTB group. The gene count is presented as circles, increasing with elevating
599 number of gene count. The significance level is presented as a color scale ($-\log_{10}(p)$).

Table legends

Table 1. Demographic and clinical data of the LTBI and NTB study population.

Table 2. Demographic and clinical data of the two drug resistant pulmonary tuberculosis patients.

Supplementary table S1. Table of 7 significantly over-represented pathways identified via the generation with the Signaling Pathway Impact Analysis (SPIA) enrichment analysis. The pathway information is based on Kyoto Encyklopedia of Genes and Genomes (KEGG) generated pathways. Global *p*-value = P_G. FDR = false discovery rate.

Supplementary table S2. Comparison of the DNA methylation status of 6 genes between our data and data from Verma *et al*. (2017) [49].

611 **Table 1.** Demographic and clinical data of the LTBI and NTB study population.

	LTBI (*N*=6)	**NTB (*N*=19)**	**Total (*N*=25)**
Age (mean)	23 (19-26)	25 (18-40)	25 (18-40)
Sex (male/female)	5/1	10/9	15/10
Weight (kg)	78.2 (54-94)	63.2 (47-85)	66.8 (47-94)
Height (cm)	175.7 (168-183)	165.4 (148-178)	167.8 (148-183)
BMI (kg/m^2)	25.2 (19.1-29.3)	22.9 (19.1-28.7)	23.5 (19.1-29.3)
Smoker/non-smoker	2/4	1/18	3/22
IGRA result (positive/negative)	6/0	0/19	6/19
History of TST-positivity (yes/no/ND)	1/4/1	3/6/10	4/10/11
BCG (vaccinated/non-vaccinated)	6/0	16/3	22/3
Included as TB-exposed/non-exposed	5/1	9/10	14/11
Previous TB-treatment (yes/no)	0/6	1/18	1/24
Previous dust exposure (yes/no)	0/6	0/19	0/25

612

613 LTBI = latent tuberculosis infection. NTB = non-tuberculosis. BMI = body mass index. BCG

614 = Bacillus Calmette-Guèrin. ND = no data. TB = tuberculosis. TST = tuberculin skin test.

615

Table 2. Demographic and clinical data of the two drug resistant pulmonary tuberculosis patients.

	DRTB (*N*=2)
Age (mean)	30 (28-32)
Sex (male/female)	2/0
Weight (kg)	61.5 (58-65)
Height (cm)	173 (166-180)
BMI (kg/m^2)	20.6 (20.1-21.1)
Smoker/previous smoker/non-smoker	0/1/1
BCG (vaccinated/non-vaccinated/ND)	1/0/1
Previous TB-treatment (yes/no)	2/0
Previous dust exposure (yes/no)	1/1
MDR-TB/XDR-TB	1/1
Smear microscopy (positive/negative)	1/1
Years of TB-disease	7 (3-11)
Duration of MDR-TB-treatment (years)	4.5 (3-6)

DRTB = drug-resistant TB. BMI = body mass index. BCG = Bacillus Calmette-Guèrin. ND = no data. TB = tuberculosis. MDR = multi-drug resistant. XDR = extensively drug resistant.

Figure 1

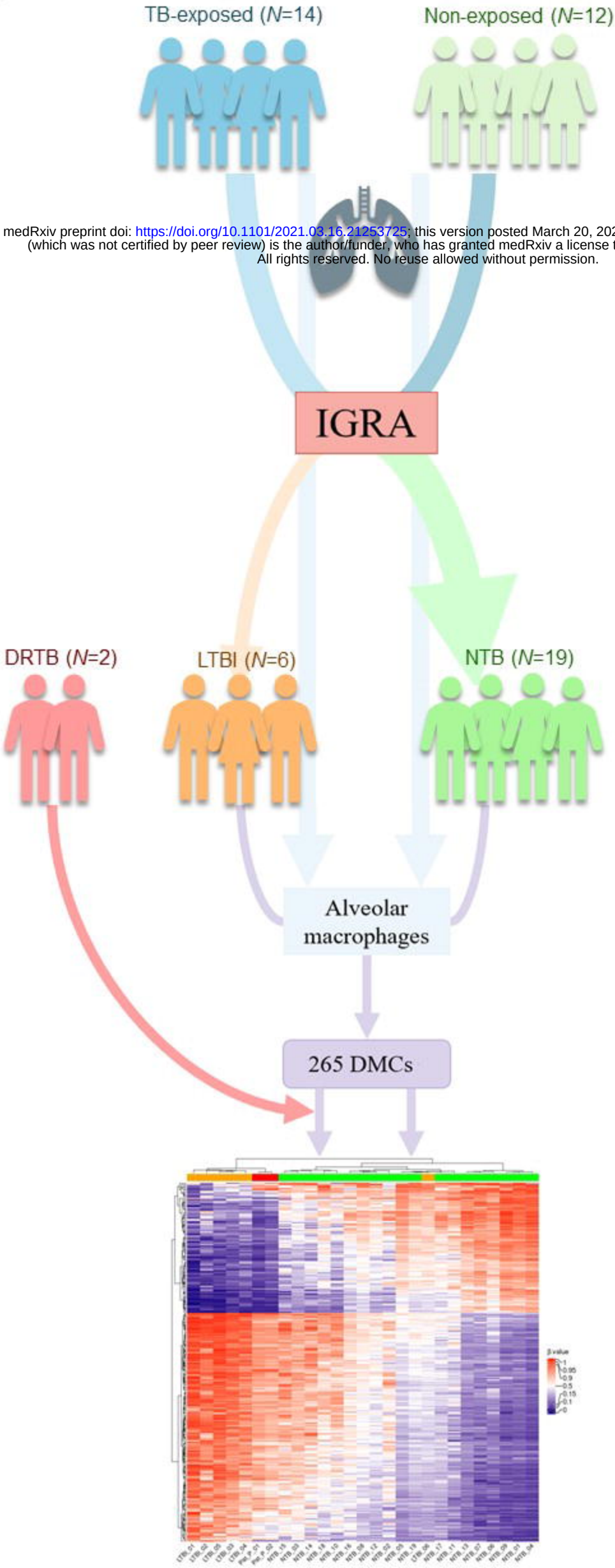

Figure 2

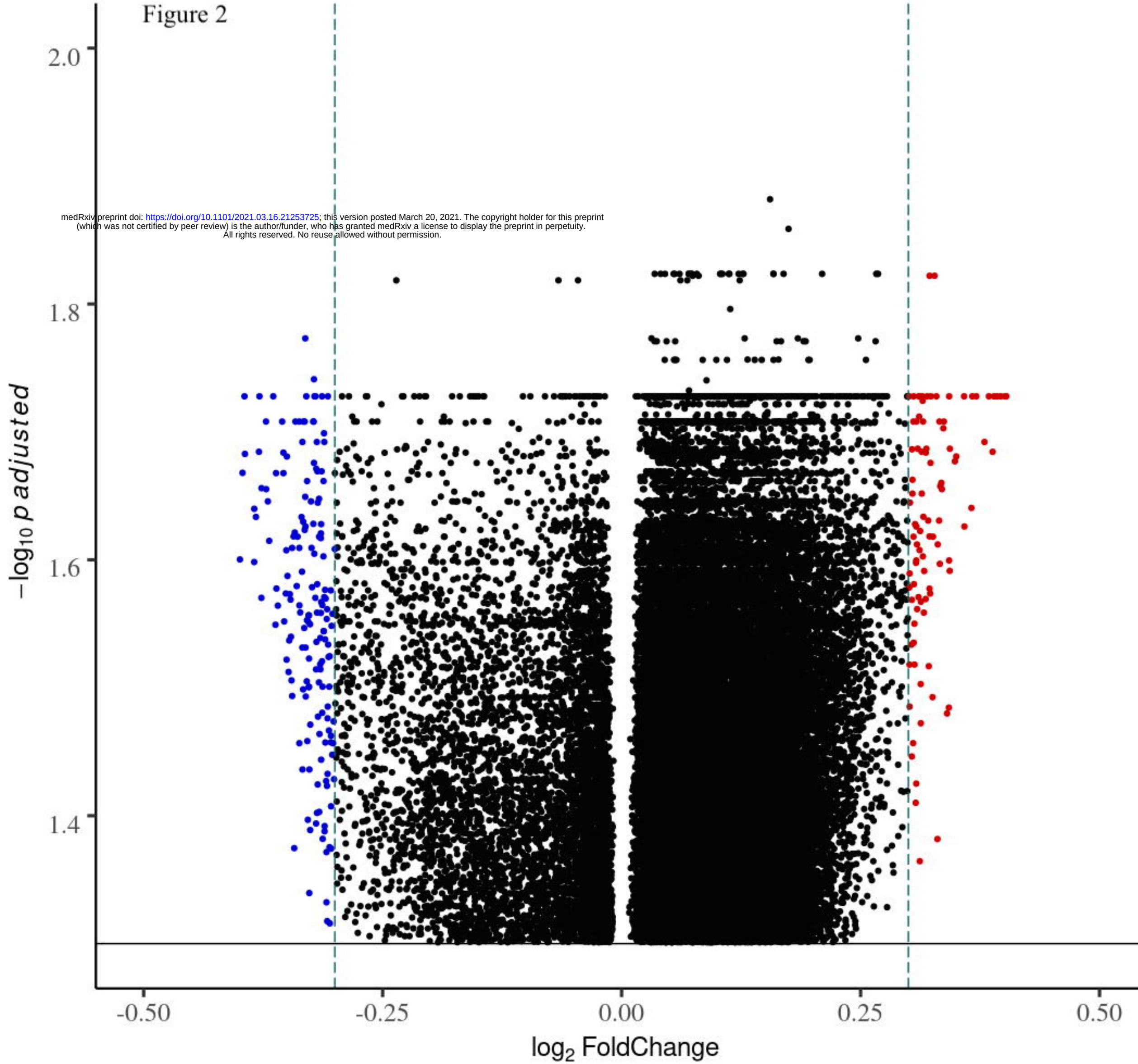

Figure 3a.

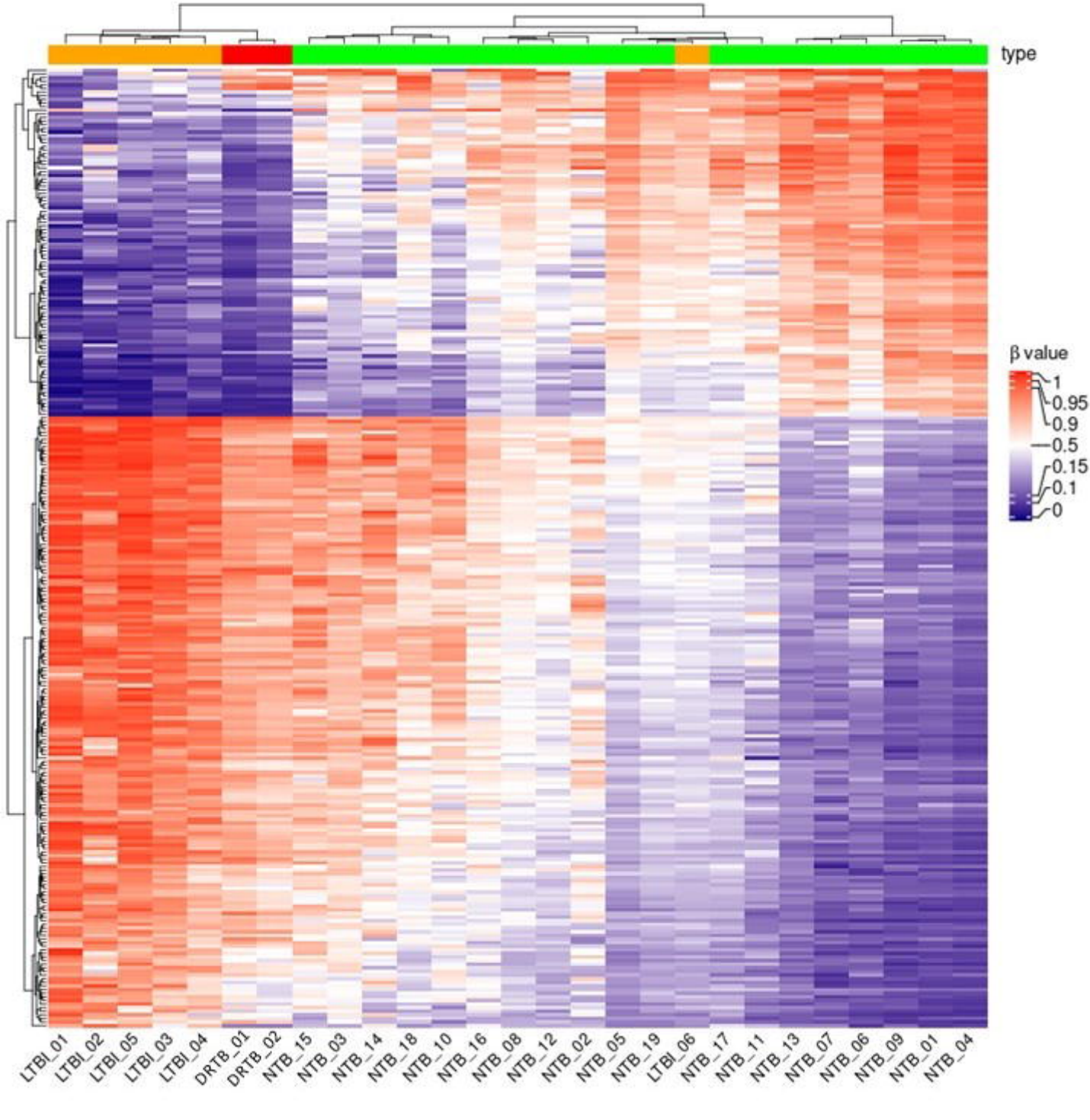
type
β value
1
0.95
0.9
0.5
0.15
0.1
0
LTBI_01
LTBI_02
LTBI_05
LTBI_03
LTBI_04
DRTB_01
DRTB_02
NTB_15
NTB_03
NTB_14
NTB_18
NTB_10
NTB_16
NTB_08
NTB_12
NTB_02
NTB_05
NTB_19
LTBI_06
NTB_17
NTB_11
NTB_13
NTB_07
NTB_06
NTB_09
NTB_01
NTB_04

Figure 3b